Processing, Thermal, and Mechanical Issues in Shape Deposition Manufacturing

F.B. Prinz, L.E. Weiss, C.H. Amon, J.L. Beuth

EDRC 24-119-95

Processing, Thermal and Mechanical Issues in Shape Deposition Manufacturing

F.B. Prinz, L.E. Weiss, C.H. Amon and JX. Beuth
Carnegie Mellon University

Abstract

An overview of Shape Deposition Manufacturing (SDM) is presented, detailing manufacturing, thermal and mechanical issues of concern in making it a commercially viable method for creating arbitrarily shaped three-dimensional metal parts. SDM is a layered manufacturing process which combines the benefits of solid freeform fabrication and other processing operations, such as multi-axis CNC machining. This manufacturing process mates possible the fabrication of multi-material layers, structures of arbitrary geometric complexity, artifacts with controlled microstructures, and the embedding of electronic components and sensors in conformal shape structures. To minimize cost, SDM is implemented using primarily commercially available hardware and CAD modeling and planning software. Important issues toward the production of high quality objects are the creation of inter-layer metallurgical bonding through substrate remelting, the control of cooling rates of both the substrate and the deposition material, and the minimization of residual thermal stress effects. Brief descriptions of thermal and mechanical modeling aspects of the process are also given. Because SDM involves molten metal deposition, an understanding of thermal aspects of the process is crucial. Current thermal modeling of the process is centered on the issue of localized remelting of previously deposited material by newly deposited molten droplets. Residual stress build-up is inherent to any manufacturing process based on successive deposition of molten material. Current mechanics modeling is centered on the issue of residual stress build-up and its potential effects, including part warping and debonding between deposited layers. Shot peening is an operation currently used to control residual stress effects and preliminary work studying its effects is also presented.*

1. Shape Deposition Manufacturing Process Description

Shape Deposition Manufacturing (SDM) (refer to Fig. 1) is a layered manufacturing process which systematically combines the benefits of Solid Freeform Fabrication (SFF) (Le., quickly planned, independent of geometry, multi-material deposition, and component embedding), with other intermediate processing operations such as CNC machining (i.e., for accuracy and precision with good surface quality), thermal deposition (i.e., to produce fully dense structures), and shot peening (Le., for stress control) (Merz et al, 1994).

Like conventional SFF processes, SDM builds shapes using a layered material deposition approach. After each layer (or layer segment) is deposited, however, the part may be transferred to other processing stations where additional operations are performed on that layer. The basic strategy is to first slice the CAD model of the shape to be fabricated into layers while maintaining the corresponding outer surface geometry information. Layer thickness varies depending on the part geometry. Each layer consists of primary material(s) (i.e., the material(s) forming the part being created) and complementary shaped

*** This wok has been supported by the Engineering Design Research Center, a NSF Engineering Research Center.**

sacrificial support structure material which is removed when the entire part is completed. Each material in each layer is then deposited as a near-net shape using thermal deposition as described below. The sequence for depositing the primary and support materials is dependent upon the local geometry and the material combinations and is also described below in more detail. After deposition, the layer is then *precisely* shaped to net shape with a 5-axis CNC milling machine or EDM, for example, before proceeding with the next intermediate processing operation or layer. The 5-axis machining eliminates the stair-step surface appearance common to conventional SFF technologies.

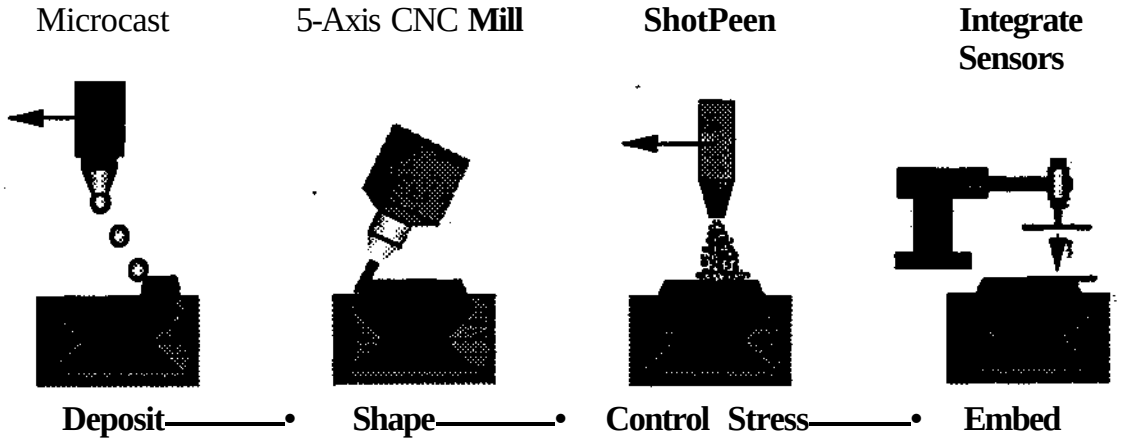

Figure 1. Shape Deposition Manufacturing

Internal residual stresses build up as each new layer is deposited due to differential contraction and thermal gradients between the freshly deposited molten material and the previously solidified layer. Internal stresses can lead to warping and to delamination. To control stress-induced warping, each layer is also shot-peened. Small round metal spheres (called 'shot') are projected at a high velocity against the surface in a blasting cabinet The complex state of stress in deposited layers makes difficult the evaluation of the effect of peening on the state of residual stress. It is clear, however, that peening imparts a compressive load which counters warping due to the net tensile load in die newly deposited top layer.

Building shapes with deposition also permits pre-formed, discrete components or assemblies to be fully embedded within the growing structure. For example, sensors can be placed throughout the structure to provide feedback for subsequent deposition process control, and when the part is operational these sensors can provide feedback on part integrity and operational parameter status.

1.1 Adaptive Shape Decomposition

In SDM there are several feasible sequences for depositing and shaping each layer. The basic sequence which we use for building a single-material part is described below and shown in Fig. 2. Variations of this sequence, which will be discussed later, may be required to improve overall process performance and part quality.

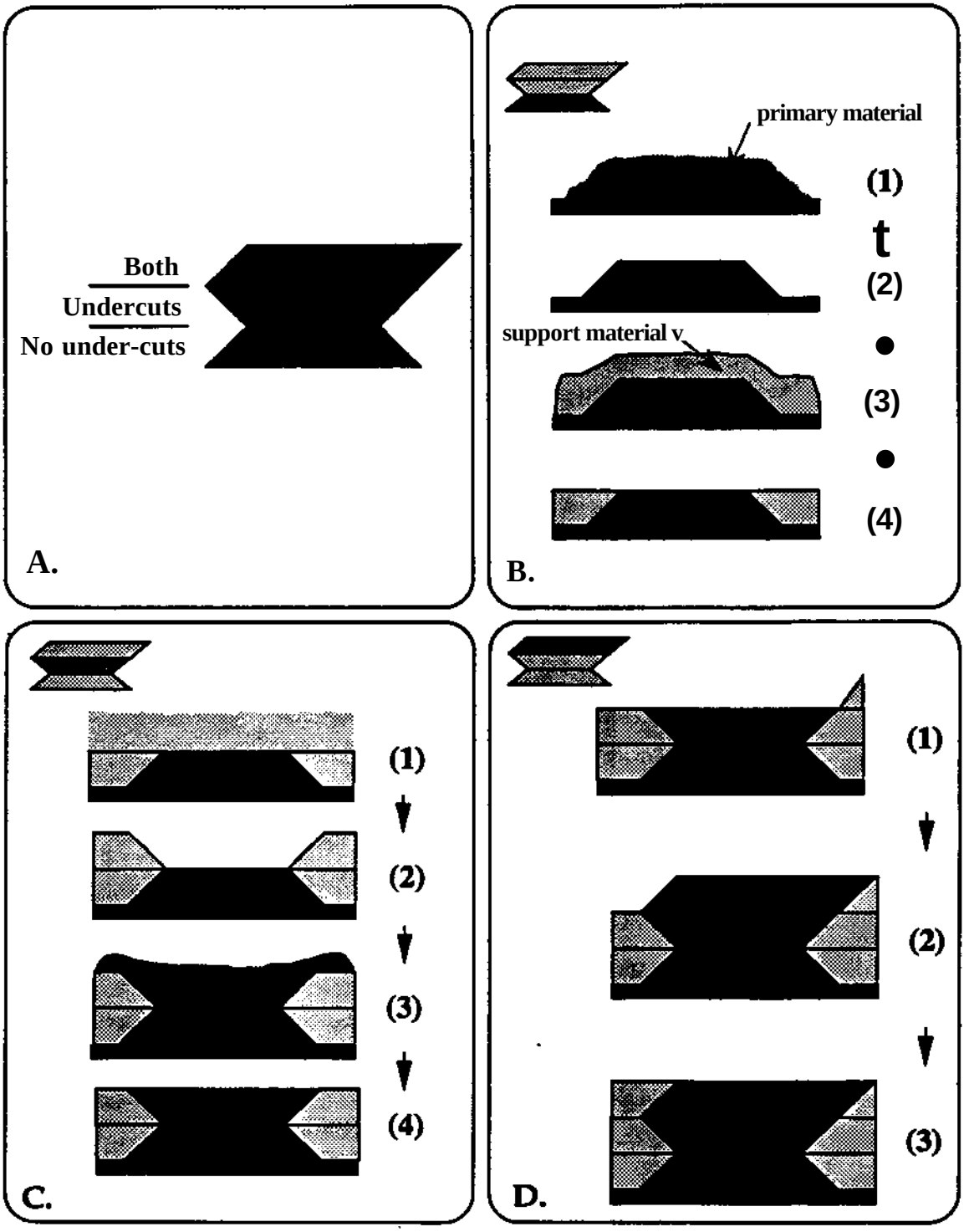

Figure 2. Sequence for depositing and shaping layers.

In general, any shape can be decomposed into layers which can be characterized by one of three categories (Fig. 2A):

- Category 1 - the layer has no under-cut features (relative to the intended building direction),
- Category 2 - the layer only has under-cut features,
- Category 3 - the layer has both under-cut and non-undercut features.

Note that straight-wall features can be considered either as under-cut or non-undercut features depending upon subtle processing steps.

The thickness of each layer will vary and the sequence for depositing and shaping the primary and support materials in each layer will also vary based upon part geometry. For layers in the first category, the primary material is deposited first (Fig. 2B, step 1) and then machined (step 2). The support material is then deposited (step 3), and the entire layer surface is planed (step 4). For layers in the second category, the aforementioned sequence is reversed (Fig. 2C).

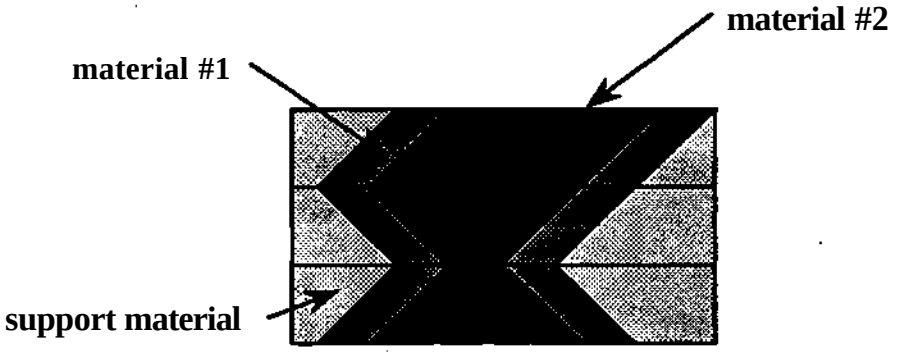

Figure 3. A multi-material structure.

Layers in the third category must be further decomposed into layer segments, or "compacts', which are deposited and shaped in a sequence such that all under-cut features (of either die primary or support materials) are formed by the previously shaped non-undercut feature. For example, in Fig. 2D, step 1, a support compact is first deposited and shaped. Then in step 2, the primary material is deposited; its undercut feature is formed by the preceding support structure compact, and its non-undercut feature is shaped by machining. In step 3, the final support material compact is deposited and similarly shaped. In general, a category 3 layer may have to be decomposed into more than three compacts and will require more than 3 steps to build. For parts which include layers with more than one material, such as depicted in Fig. 3, each of these layers are simply built according to the category 3 sequence described above.

1.2 Thermal Deposition

One goal for SDM is to be able to *directly* create fully dense metal structures with a controlled microstructure. One way to achieve densification is to melt and to superheat the deposited material such that it remelts and fuses with the previously deposited and

solidified material. Conventional welding, such as MIG, TIG, or plasma accomplishes this. However, since the arc is transferred to the substrate, the local temperatures are excessive which may destroy the shape and microstnicture of previously deposited material. Conversely in thermal spraying (which has been previously implemented within SDM), such as arc or plasma, the arc is not transferred to the substrate so that the sprayed material does not, in general, destroy the underlying shape or microstnicture. The sprayed molten droplets, however, are very small and do not contain enough heat to form metallurgical bonds (i.e., post-processing such as HEPing or sintering is required) upon solidification.

A process is required which combines the benefits of welding (i.e., metallurgical bonding) with thermal spraying (i.e., controlled heat transfer to substrate). 'Microcasting' is a non-transferred welding process (Fig. 4) which we are developing for this purpose. In microcasting, an arc is established between a conventional plasma welding torch and the feedstock wire. The wire may be fed from a conventional MIG torch for example. The wire melts in the arc forming a molten pool on the end of the wire. A discrete droplet falls off of the wire when the molten material is heavy enough to overcome the surface tension by which it adheres to the wire. The droplet then accelerates to the underlying substrate by gravity. In contrast to the small droplets created with thermal spraying (i.e., on the order of 10|im in diameter), microcast droplets are much larger (i.e., on the order of 10mm diameter). The larger microcast droplets remain superheated in flight and contain sufficient energy to *locally* remelt the underlying substrate. The rapid solidification of molten droplets onto colder substrates allows for fusion bonding of dissimilar materials even for cases where a higher melting material is fused on top of a material with lower melting point temperature. For on example, we have built parts out of 316L stainless-steel using copper support material. The copper is sacrificed from the completed shape using nitric acid.

To control oxidation, it is critical to shield the droplets and substrate with inert gas. Placing the microcaster in an environmental chamber is feasible, but costly. Alternatively, it is straight-forward with this process to locally shroud the droplets and working area with inert gas. For this purpose we use a commercial, proprietary shrouding apparatus.

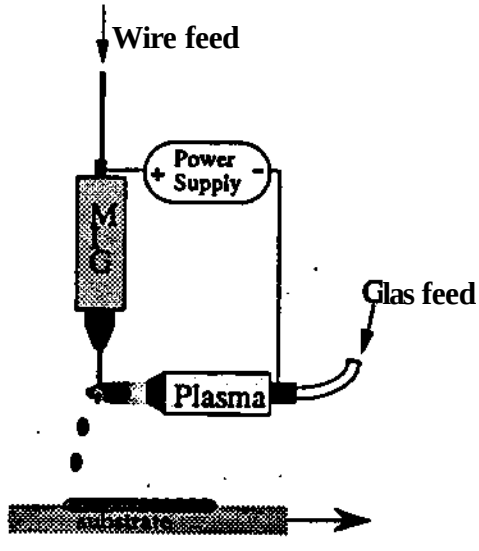

Figure 4. *Microcasting.*

A key advantage of the microcasting process stems from its low operational cost as well as the commercial availability of components such as plasma welding torch, power supply, wire feed mechanisms, and inerting shrouds. Other thermal deposition processes, such as laser welding may also be suitable for SDM.

1.3 System Implementation

One of our goals is to implement SDM in such a way that is both economical and flexible. To minimize costs we use primarily *commercially available* apparatus integrated in novel arrangements, such as the microcaster described above. Custom equipment has signiflcant development and production costs and does not have the factory support available for mature processes. By flexibility we mean the ability to easily add and investigate different deposition, shaping and intermediate processes. For this purpose we currently build our parts on pallets and use robotic automation to transfer the pallets to the different processing stations (Fig. 5). Each station has a pallet receiver mechanism which locates and clamps the pallet in place. The deposition station also uses robotics to integrate multiple deposition processes.

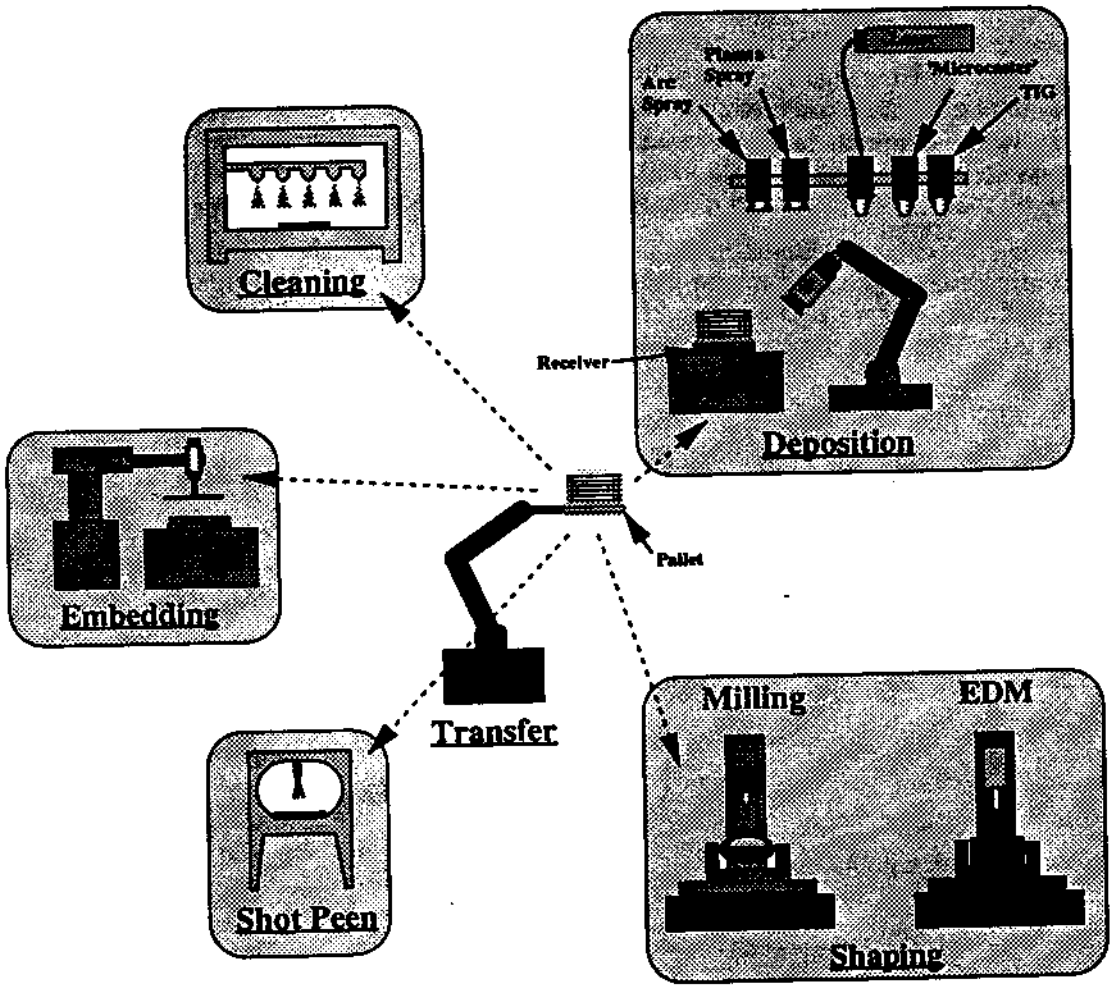

Figure 5. *Shape Deposition Manufacturing facility.*

Given a CAD model of the desired part, a CAD/CAM planning and control system is required for the SDM process to automatically:

- slice adaptively the part,
- determine the manufacturing steps necessary to build the part,
- generate the cutting trajectories for CNC machining operations,
- generate paths for material deposition,
- generate the code required to run the cell, and
- execute the commands on the individual stations.

We are currently developing a planner based upon the ACIS geometric modeling kernel. The CAD models are nonlinear representations which ultimately lead to better accuracy and surface quality than can be achieved with linear representations. Translators to convert CAD models produced by major commercial CAD systems (e.g., PRO-E, IDEAS, AUTOCAD) to ACIS representations exist or are currently being written.

2. Thermal Modeling of Microcasting Process

The achievement of an accurate thermal model is an important step toward making SDM viable by virtue of determining the conditions needed for complete bonding of the droplet and substrate, for protection of support structures and embedded sensors, and for controlling thermal-induced residual stresses. A one-dimensional, mixed Lagrangian-Eulerian thermal model of the microcasting process has been developed and used extensively to explore the operating conditions available for the deposition of superheated liquid metal droplets onto a solid substrate (Amon et al, 1994a). The heat transfer model includes temperature dependent properties and pure metal phase change phenomena, but excludes droplet dynamics; it is capable of tracking the melting front location both in the droplet during solidification and into the substrate during remelting. A lumped parameter time scale analysis has been applied to validate the assumptions required for the initial numerical model (Amon et al, 1994b). Using this model, it has been possible to investigate the likelihood of remelting and the sensitivity of remelting to droplet and substrate conditions, as well as predict droplet and surface temperatures and cooling rates.

The microcasting deposition equipment has been modified over the past year, including the addition of shrouding equipment to lessen the extent of droplet oxidation and alterations to the plasma gas composition to improve deposition quality. Different materials have been explored for consideration as both the artifact and sacrificial support material, being stainless steel and copper respectively the current choices. Numerical simulations have been performed for the various new combinations at each step of the process evolution. Verification of the numerical results has been accomplished through the formulation of an analytical solution which is valid in certain range of process parameters and conditions (Amon et al, 1994b). Experiments have also been performed along the way to further validate the numerical results and to determine the correct initial conditions needed for the numerical modeling. Calorimetry tests have been performed on the microcasting equipment to measure the average impacting droplet temperatures over a wide range of application parameters; thermocouple measurements of droplet and substrate temperatures have recorded transient temperatures for typical microcasting conditions; and metallographic examination of several of test samples have ascertained remelting depths and material microstructures.

2.1 **Temperature** Prediction of the Droplet **and Substrate**

The generation of an analytical formulation of the temperature and remelting process was performed using simplifications such as constant material properties and constant temperature boundary conditions. While it is only applicable for the microcasting process over the initial 0.01 second time span of the deposition process, this formulation does permit the comparison of numerical predictions with analytical results over the initial remelting period. This initial remelting phenomenon is completed in too brief a time period to be investigated using thermocouple experimental techniques. The analytical formulation also provides a method for calculating the initial temperature at the droplet/substrate interface. This has allowed the exploration of the temperatures required either for the impacting droplet or for the substrate in order to achieve substrate remelting in both similar and dissimilar deposition applications. The latter is particularly useful for calculating the conditions present when sacrificial support material and artifact material surfaces are in contact; based on these calculations, it is possible to remelt a stainless steel substrate with a stainless steel droplet, without remelting a copper substrate material. These analytical results are summarized in Fig. 6, showing the temperatures (droplet and substrate) required to achieve interface bonding through remelting. For example, a 2300 °C stainless steel droplet would cause remelting with a 150 °C stainless steel substrate, but remelting a copper substrate would require a substrate temperature in excess of 200 °C. Similarly, it is possible for a copper droplet to remelt a copper substrate without remelting a stainless steel substrate. The temperatures needed for these effects are available with the microcasting equipment

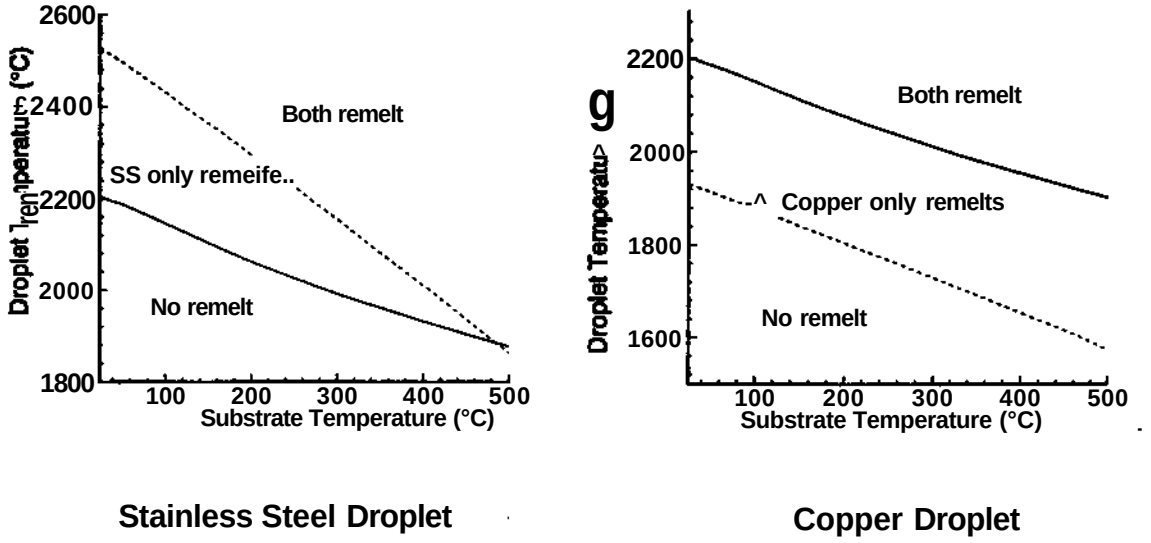

Figure 6. Initial Interface Temperatures for Stainless Steel/Copper Deposition.

2.2 Experimental Temperature Measurement and Substrate Remelting

Calorimetry experiment results have determined the average impact temperatures for stainless steel droplets over a wide range of application feed rates and heat source power settings. An average impact temperature of 2300 °C was used for the model, and the microcasting equipment settings can be altered to change this by 800 °C over the range of

parameters explored. Copper droplets have an average impacting temperature of 2000 °C, and a range of about 600 °C.

Thermocouple experiments have been performed to determine both individual droplet temperatures (directly impacting a droplet onto a thermocouple) and substrate temperatures (inserting thermocouples nearly through the substrate). Measurements have also been collected at lateral distances from the droplet impact, using the same substrate depths, to further determine the substrate temperature distributions. Thermocouple experiments and numerical simulations have been compared, using the measured droplet temperatures as initial conditions for the model, and the cooled droplet "splat" height for model dimensions. Figure 7 shows the comparison of thermocouple measurements and numerical predictions for a stainless steel droplet impinging on a stainless steel substrate. The cooling rates predicted by the model are initially comparable to the experimental results; however, the simulated results, at later times, reflect a smaller cooling rate than measured by experiments. Numerically calculated substrate temperatures are greater than the results from the thermocouple measurements. The numerical underprediction of droplet cooling and overprediction of substrate heating is expected because the model only considers one-dimensional heat fluxes, while the actual process is multi-dimensional.

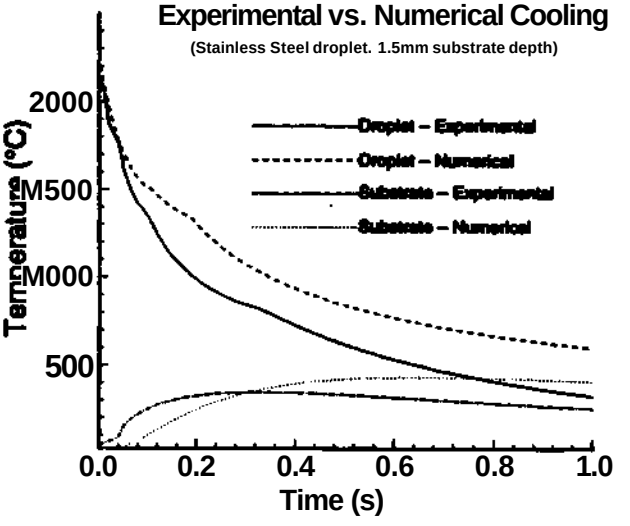

Figure 7. Numerical vs. Experimental Temperatures for a Stainless Steel Droplet.

Determination of actual substrate remelting, which occurs in about 10^{-5} seconds, has been verified by metallographic examination of the sample plates used for the substrate temperature experiments. This enables us to correlate the observed remelting with measured temperatures and cooling rate predictions. Carbon steel droplets exhibit martensitic and ferrite microstructures indicative of the rapid cooling of the droplet, and a microstructure grain orientation perpendicular to the droplet/substrate interface which indicates that the heat flow is predominantly into the substrate. The substrate plate undergoes both remelting and solid state transformations, where the original plate's ferrite-pearlite structure becomes increasingly fine as the droplet is approached. The curved shape of the heat affected substrate zone clearly shows that substrate heat transfer is multi-dimensional. Remelting yields martensite, lower bainite, and carbide inclusions, but the accurate measurement of remelting depth is difficult to determine due to the solid state transformations. Cooling rate estimates can also be made from the microstructure examination using carbon steel cooling transformation diagrams.

In addition, a continuously deposited series of droplets was examined by metallography, which reflects more accurately the actual SDM process, and the preheated substrate conditions that occur during manufacturing. These tests indicate that the remelting depth does not appreciably change as the substrate is heated by previous droplets to a few hundred degrees. The occurrence of gas voids at the interface does decrease as the substrate is heated. This will improve the heat transfer process, as well as resulting material properties.

Metallographic examinations performed on the stainless steel samples allow more accurate determination of the remelting depth, because the austenitic stainless steel used for deposition does not undergo solid state microstructure transformations at the peak temperatures and elevated temperature durations present with microcasting. The micrograph tests indicate that a remelting depth of 10 microns exists for the microcasting deposition condition which is in good agreement with the numerical model prediction.

Comparison of the measured results with the existing numerical simulations shows that the one-dimensional simplification can provide useful information regarding the initial stages of the substrate remelting and droplet solidification as well as a qualitative understanding of the microcasting process, but it is only modestly successful in matching experimental temperature tests over an extended time. In particular, while the droplet heat flow is predominantly one-dimensional towards the substrate, the substrate cooling is not. Including fluid dynamics and two-dimensional heat transfer into the model is required for improved accuracy in the predictions. Some existing numerical models have used an effective, droplet-substrate heat transfer coefficient to account for the heat transfer into the substrate (Trapaga et al, 1992). However, this coefficient has been calculated using our numerical simulation results, and found to vary considerably during the substrate remelting process (Amon et al, 1994b). Consequently, the heat transfer from the droplet to the substrate will have to be determined by a conjugate droplet convection/substrate conduction formulation.

A spectral element (higher-order finite element formulation) method has been selected for the performance of multi-dimensional thermal simulations that include the motion of the droplet This technique is well suited for free surface flows and offers the capability of rapid convergence and the ability to include time-varying properties over a complex domain shape. Current work involves the evaluation of existing solidification models to accurately model alloy solidification which takes place over a temperature range and includes diffusion effects, and the understanding of the fluid dynamics at the droplet/substrate interface. In addition, experimental tests are being performed in an effort to optimize the manufacturing parameters, to reduce the voids formation and to improve the artifact quality.

3. Residual Stress Modeling and Control

In this section, the issue of residual stress build-up in shape deposited parts is addressed. In addition, specific undesirable consequences of residual stresses are studied as are methods currently used to control them. Residual stresses can lead to reduced apparent strength or life in manufactured parts. This is of particular concern in parts that must withstand substantial mechanical or thermal applied loads. In addition, residual stresses can lead to a number of undesirable effects that are of concern even for parts without significant applied loading in their application. These effects include part warping (curvature), loss of edge tolerance, and, in multi-material parts, residual stress-driven inter-layer debonding. Residual stress build-up is inherent in any manufacturing process based on successive molten material deposition. The goal of this work is to understand residual stresses and therefore limit their magnitudes and their unwanted effects through process changes and changes in part designs.

Research into residual stress modeling and control has addressed three topics:

1) Residual Stress Modeling: Uncoupled heat transfer and mechanical analyses (preliminary models) have been developed to predict residual stresses in microcasted droplets.
2) Debonding Between Layers: Methods have been developed for predicting residual stress-driven inter-layer debonding in multi-material parts.
3) Shot Peening: Initial tests have been performed to determine the effect of shot peening on manufactured parts. Preliminary conclusions have been arrived at

3.1 Residual Stress Modeling

The immediate goal of this work is to accurately model solidification and residual stress build-up on a droplet level. A longer-term goal is to be able to scale up results on a droplet level to predict residual stresses throughout an entire microcasted part This work requires uncoupled heat transfer and mechanics models, with temperatures as a function of time and location from the heat transfer analysis used as inputs to the mechanics solution. The approach taken is similar to that used to model residual stresses in casting problems by, among others, Zabaras, Ruan, and Richmond, 1991. The initial heat transfer model used is an analog of the one-dimensional model outlined in the previous section on thermal modeling. It has been determined that the most efficient method of linking the heat transfer and mechanics analyses is to solve both problems using ABAQUS finite element software.

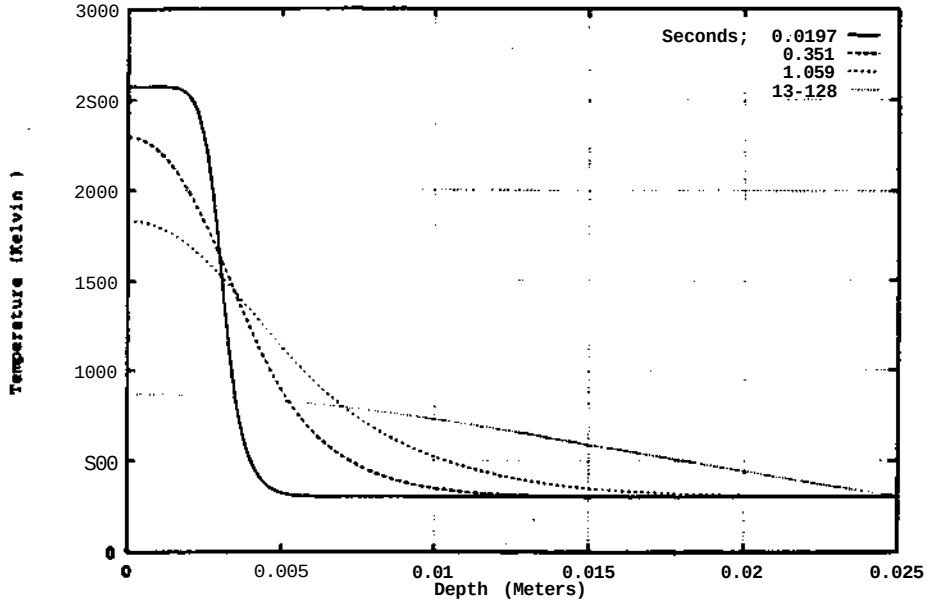

Figure 8. Temperature vs. depth at discrete times during cooling.

Research into residual stress build-up in parts created using SDM has included the following:

- The one-dimensional droplet-level heat transfer problem was re-solved using ABAQUS finite element software.
- The finite element temperature results were verified against results from the thermal solution presented in Section 2 on thermal modeling.

- **Temperatures as a function of time and location were inserted into axisymmetric mechanics analyses.**
- **Stresses as a function of time and location were obtained. The stress models developed thus far include temperature-dependent properties, including temperature-dependent yield stress and secondary creep deformation.**

As an example of the results that have been obtained from this work, Fig. 8 provides a plot of temperature vs. location through the "droplet" and "substrate" thicknesses at various times during the cooling process, as modeled using the 1-D finite element heat transfer model. The total depth of the droplet/substrate is 25 mm. The initial interface between the liquid and solid is at a depth of 3 mm. These results agree with temperature data from the 1-D thermal model of Section 2. Figure 9 gives a corresponding plot from the finite element solid model of normalized axial stress at discrete times vs. location under the simplified assumptions of temperature-independent elastic behavior. This type of simplified model is useful in understanding the results for more complete analyses with temperature-dependent properties. The results for the final stresses in each portion of the model agree with simple hand-written calculations based on ocAT, E and v.

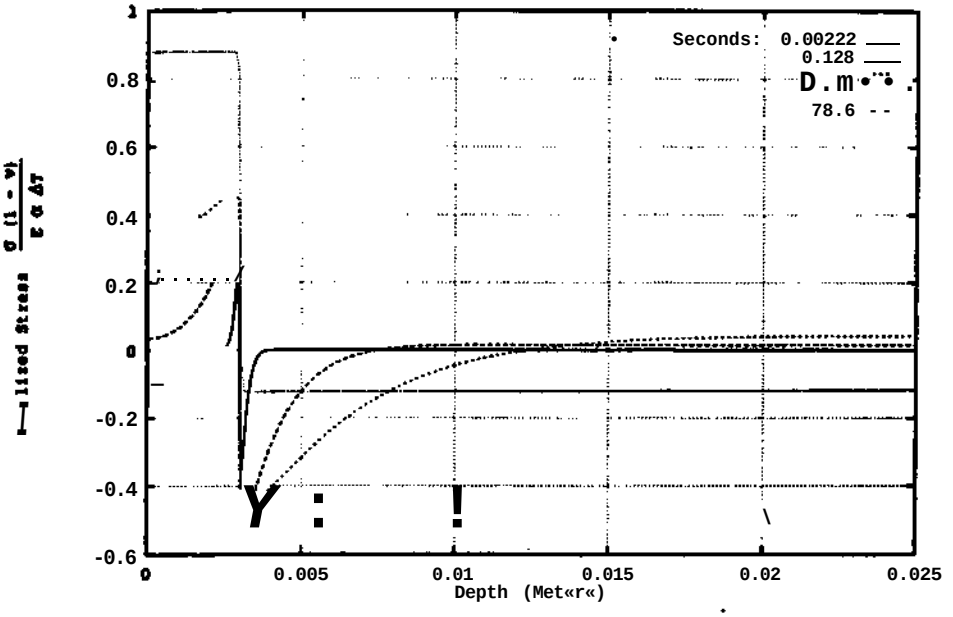

Figure 9. *Normalized axial stress vs. depth at discrete times during cooling for temperature-independentelasticmechanicalproperties.*

Predicted stresses as a function of depth have also been obtained for the case of temperature dependent properties, including yield behavior and secondary (steady-state) creep. Figure 10 gives a typical result for the stresses through a single solidified drop of stainless steel deposited onto a stainless steel substrate. In this particular set of results a temperature-independent axial yield stress of 300 MPa is assumed. A few conclusions can be offered based on the results shown in Fig. 10 and other preliminary results. One is that the stress state in the top portion of the existing (substrate) material is changed drastically by thermal cycling from newly applied droplets. Specifically, the results given in Fig. 10 indicate that originally unstressed regions below the deposited droplet go through a compression/tension elastic-plastic thermal stress cycle. A second point is that the final stresses in a deposited droplet will be at or near the material yield stress. It should be noted that the modeling thus far has been for a single droplet deposited onto a thick substrate, simulating the effect of

droplets of a manufactured part being deposited onto a thick pallet The results given in Fig. 10 suggest that residual stresses near the yield point are likely during part manufacture. It is likely that these stresses will be substantially relaxed, however, once the part is completed and is removed from the pallet upon which it is built

Future work in this area will include two-dimensional modeling of the thermal and mechanical problems, to capture two-dimensional aspects of heat conduction into the substrate material and to better model mechanical constraints imposed on deposited droplets. Because these models will require assumptions concerning droplet shape, the thermal modeling will be perfbrmed in parallel with the spectral element thermal model (see Section 2) currently under development to predict droplet temperatures and shape. Both thermal and mechanical results will be compared with experiments. Predicted temperatures will be compared to results from thermocouple measurements. Predicted residual stresses will be compared to surface residual stresses measured using x-ray diffraction.

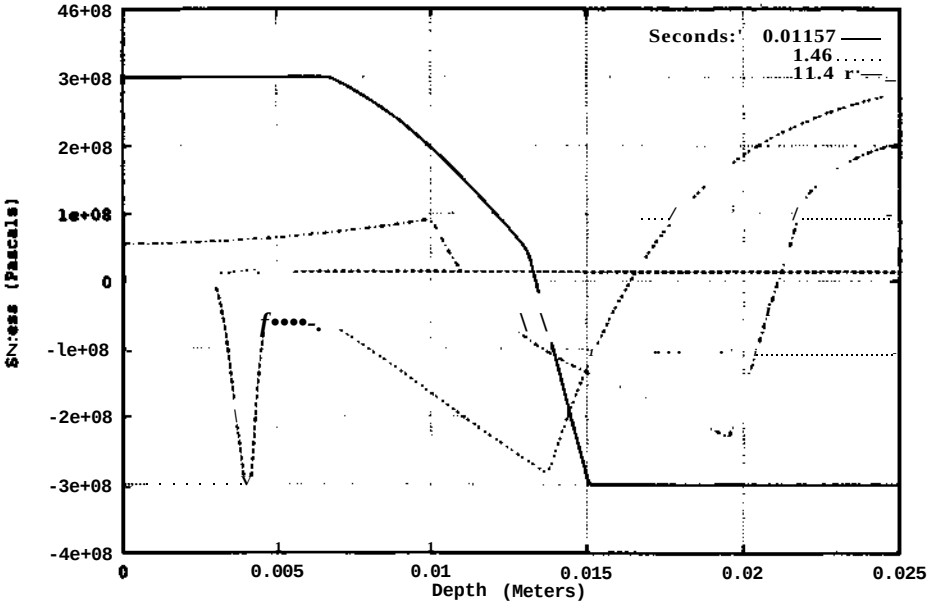

Figure 10. Axial stress vs. depth at discrete times during cooling using a mechanics model accounting for yielding and temperature-dependent secondary creep.

3.2 Debonding Between Layers

As noted in Section 1, microcasting is the thermal deposition process currently used in SDM. A major goal in pursuing microcasting has been to increase bonding between layers as compared to previously used thermal spraying techniques. In making a transition from spray-based thermal deposition to microcasting, the degree to which inter-layer debonding is observed in manufactured parts has been substantially reduced. In particular, for parts made entirely of stainless steel, an "interface" between deposited layers typically does not exist in microcasted parts. Depending on processing conditions, deposition of copper onto copper can lead to debonding between deposited layers because the high thermal conductivity of copper causes very rapid cooling of deposited drops. For example, some debonding has been observed between layers of copper support material, which can lead to a loss of constraint in a part as it is built Principal concerns related to inter-layer debonding are associated with multi-material parts, where control of re-melting conditions

may be difficult. In theory, for a large number of material combinations, one could make droplets of one material hot enough to fuse well with whatever material they are being deposited onto. In practice, however, there is an inherent competition between obtaining enough remelting for a good bond but not so much remelting that machined features such as edges and corners are affected. In the application of multi-material parts created via layered manufacturing methods, the possibility of debonding along interfaces between materials will necessarily be a design concern.

Research in understanding inter-layer debonding has centered on identifying an energy release rate quantity as the critical driving force for residual stress-driven delamination (Beuth and Narayan, 1994, 1995). The identified energy release rate can be calculated without having to resort to full fracture mechanics-based finite element (or other) modeling. The goal is to use this energy release rate quantity as a means to evaluate potential part designs for their susceptibility to debonding.

As an example, Fig. 11 gives a diagram of a four-layer part that is debonding along its midplane interface. The debond is propagating with a crack length, a, measured from the left edge of the part. The type of part to be considered here will be made of alternating layers of two different materials. In current debonding models, a simplified model of residual stresses is used. It is assumed that each layer of the part has experienced a uniform "free thermal" contraction relative to the layer below it In the particular cases considered here, it is assumed that the free thermal strain mismatches between layers are equal in magnitude. The methods developed to predict debonding can also be used in conjunction with the more precise residual stress solidification models under development

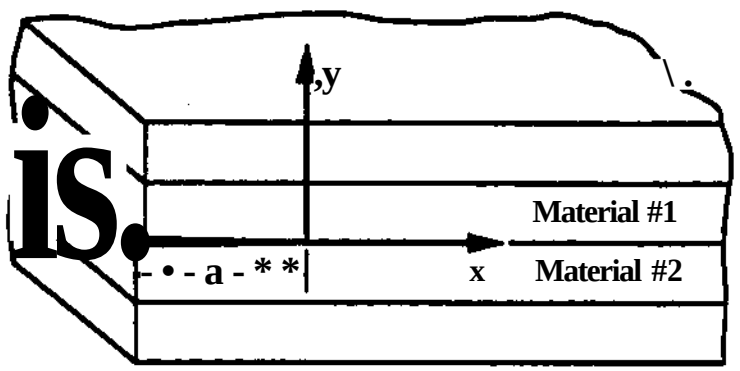

Figure 11. *Debonding of a four-layer part along its midplane interface.*

Two-dimensional finite element analyses of the type of delamination problem illustrated in Fig. 11 have been carried out, treating the problem as an interfacial fracture mechanics problem. Figure 12 gives a plot of normalized energy release rate of a delamination crack as a function of normalized crack length. The case presented is that of a single stiff layer debonding from the bottom of a 4-layer part consisting of alternating stiff and compliant layers of equal thickness. The layers have a ratio of stiffnesses equal to 1:3. A symmetric model is used with a half-length equal to 25 layer thicknesses, h. The plot in Fig. 12 shows that the energy release rate reaches a constant (steady-state) value for crack lengths on the order of 3 or more layer thicknesses, h. Furthermore, this steady-state value of G can be calculated without using a fracture model of the problem. Instead, a model of the residual stresses in a fully bonded part can be used. Such steady-state values of G (designated as G_{ss}) exist for delamination along any interface in such a part and a methodology has been formulated for calculating them.

In addition to analyses calculating the driving force behind debonding, preliminary measurements of interfacial toughnesses (resistances to debonding) have been made for microcasted copper-stainless steel interfaces. The goal of this work is to compare steady-state G values with critical values of G (i.e. measured toughnesses) for each interface. If the critical G, G_c, for an interface is greater than the steady-state G, G_{ss}» then no delamination is predicted to occur on that interface. In part designs where the G_c values for all interfaces are comparable, Gss values can be used by themselves to rank designs for their susceptibility to delamination.

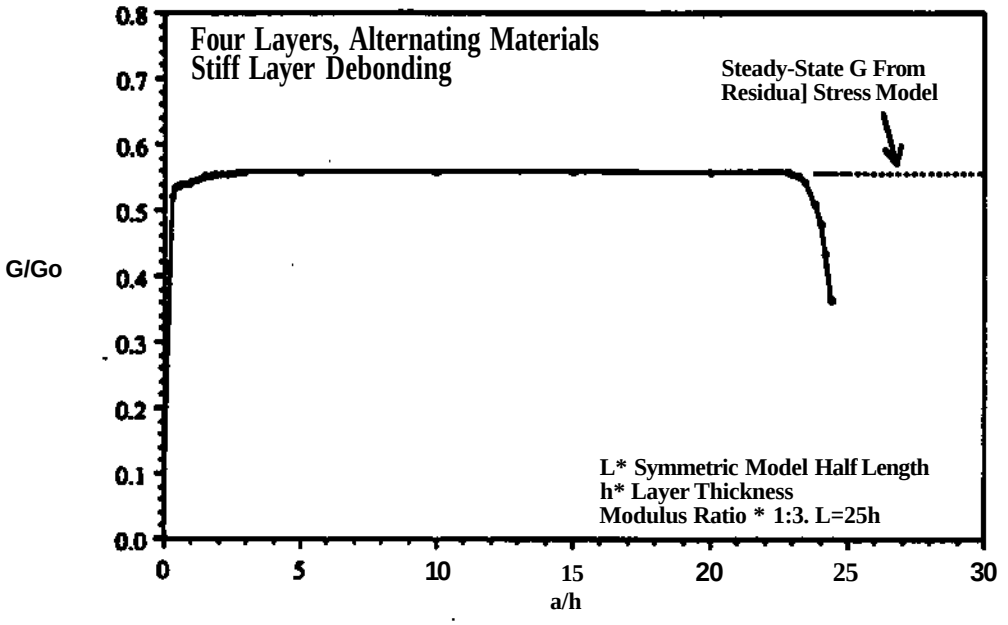

Figure 12. *Normalized energy release rate of a delamination crack vs. normalized cracklength.*

3.3 Shot Peening

The goals of research into shot peening are to determine qualitatively the effects of peening on part warping and stresses and to predict quantitatively how much peening is required to achieve a desired shape change. A set of preliminary tests has been completed. Coupons of annealed 304 stainless steel with dimensions 20.32 cm in length and 1.91 cm in width were tested. Specimen thicknesses of 0.470 cm, 0.63S cm and 0.914 cm were tested. A shot diameter of 0.165 cm was used with a standard operating pressure of 221 kPa. Axial strains measured on the bottom of each specimen were recorded as a function of the number of passes of the shot peener over the specimen.

The effect of peening has been modeled as a net free dilatation strain (expansion) of a thin layer of material (the peened layer) relative to the layer below it (the rest of the specimen). The dilatational strain caused by the shot peening is analogous to a uniform thermal expansion in the peened "layer". Elastic-plastic beam-based and finite element analyses have been used to calculate the free strain of the peened layer, using measured strains on the bottom of each specimen.

Figure 13 gives a plot of free dilatational strain in the peened "layer" vs. measured axial strain on the bottom of the specimen for the three test geometries. Points are the experimental values, measured after each pass of the shot peener. From the plot, it is clear that the effect of peening for a given number of passes is a function of specimen thickness. In addition to the fact that the thicker specimens deform less because of their higher stiffness, thicker specimens actually exhibit smaller free strains due to peening for the same number of passes. Also, for the thicker specimens, although a significant amount of free strain occurs in the first pass of the peener, subsequent passes do not increase the free strain as much. Both of these effects are related to the higher level of constraint in the thicker specimens. The thicker specimens build up higher net biaxial compressive stresses in the shot peened layer. This higher in-plane compressive stress inhibits plastic deformation (net free dilatational strain) due to peening during the first pass and particularly after the first pass.

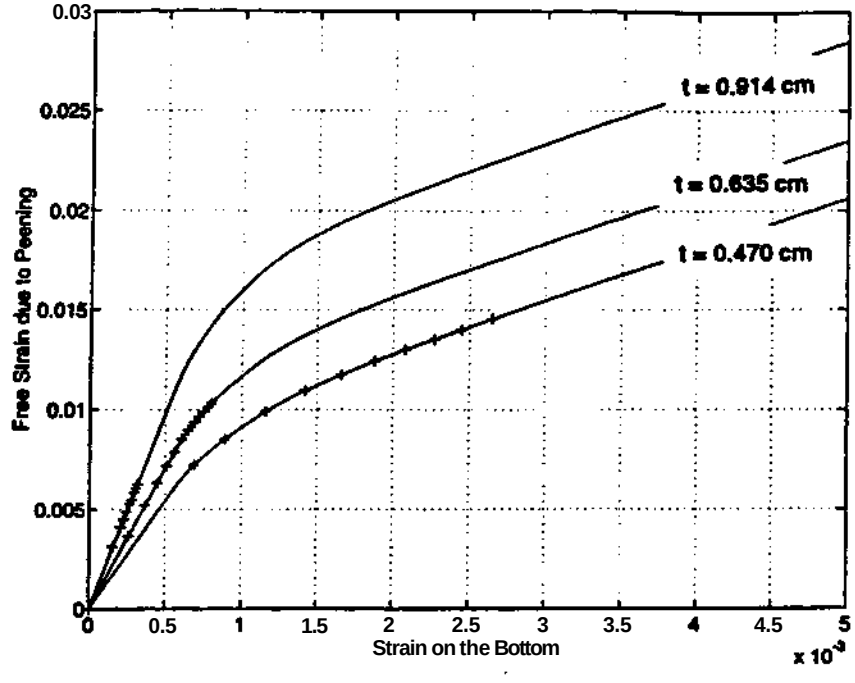

Figure 13. *Free strain due to peening vs. measured axial strain.*

Based on the results of tests conducted thus far, several qualitative conclusions can be drawn concerning the effectiveness of using shot peening to produce shape changes in shape deposited parts. First, most of the effect of shot peening on part shape may come after a single shot peening pass. Subsequent passes may have little additional effect on the part Second, the level of constraint in the part being peened is important, as are residual stress levels in the top of the layer before peening. Just as a thicker specimen experiences a smaller free strain per pass than a thinner specimen, a fully constrained part will be less affected by shot peening than an unconstrained part Conversely, residual tensile stresses in the top layer of a part before it is peened will cause that part to be more affected by shot peening than it would be without tensile residual stress. Finally, the possibility of multiple peening passes producing too much shape change in manufactured parts should not be a concern. The build-up of compressive stresses in constrained parts places a limit on shape changes that can be achieved after the first few passes of the shot peener.

Summary

A review of manufacturing, heat transfer and solid mechanics research issues of Shape Deposition Manufacturing (SDM) has been presented. Research efforts related to each disciplinary topic are highly interconnected even though they have been presented separately. For example, residual stress modeling depends upon spatial-temporal temperature evolution obtained from the thermal models, and inter-layer debonding is inherently linked to substrate remelting. Important factors that control the quality and material properties of the parts fabricated by SDM are the cooling rates which determine the microstructure, the metallurgic bonding which is affected by substrate remelting and the residual thermal stress build-up which may induce part warping and debonding between deposited layers. Therefore, the understanding of SDM thermal and mechanical effects has two major goals: first, to aid in the selection of improved SDM process parameters, and second, to enable the integration of models under development with the SDM C AD-based design system. The furthest objective of this combined effort is to allow SDM to become a feasible and cost-effective method for creating arbitrary three-dimensional shapes with multiple materials and for embedding sensors and electronic components in complex structures.

Acknowledgement

The authors gratefully acknowledge the Office of Naval Research, Grant No. N00014-94-1-0183, the Advanced Research Project Agency, Grant No. JFBI92195, the University Research Initiative at the University of California, Santa Barbara, Grant No. N00014-92-J-1808 and the Engineering Design Research Center, an Engineering Research Center of the National Science Foundation, Grant No. EEC-8943164.

References

Amon, C, Beuth, J., Kirchner, H., Merz, R., Prinz, F., Schmaltz, K. and Weiss, L. (1993) "Material Issues in Layered Forming," ***Proc. 1993 Solid Freeform Fabrication Symp.,*** **eds. H.L. Marcus et al., pp. 1-10, Austin, TX.**

Amon, C.H., Finger, S., Prinz, F.B. and Weiss, L.E. (1994a) "Modeling Novel Manufacturing Processes," ***International Mechanical Engineering Congress and Exposition, ASME 1994 IMECE,*** **Chicago, Illinois. In** ***Manufacturing Science and Engineering,*** **ASME-PED, Vol. 68-2, pp. 535-546.**

Amon, C.H., Merz, R., Prinz, F.B. and Schmaltz, K.S. (1994b) "Thermal Modelling and Experimental Testing of MD* Spray Shape Deposition Processes," ***Proc. l(f^h International Heat Transfer Conference,*** **Vol. 7, pp. 321-327, Brighton, UK.**

Beuth, J.L. and Narayan, S.H., (1994) "Residual Stress-Driven Delamination in Shape Deposited Materials," ***Mechanics in Materials Processing and Manufacturing*** **(TJ. Moon and M.N. Ghasemi Nejhad eds.), Proc. International Mechanical Engineering Congress and Exposition, Chicago IL, ASME-AMD, Vol. 194, pp. 19-34.**

Beuth, J.L. and Narayan, S.H. (1995) "Residual Stress-Driven Delamination in Deposited Multi-Layers," accepted for publication in the ***International Journal of Solids and Structures.***

Merz, R., Prinz, F.B., Ramaswami, K., Terk, M., and Weiss, L.E. (1994) "Shape Deposition Manufacturing," ***Proceedings Solid Freeform Fabrication Symposium,*** **H. Marcus, JJ. Beaman, J.W. Barlow, D.L. Bourell and R.H. Crawford eds., The University of Texas at Austin, pp. 1-8.**

Trapaga, G., Matthys, E.F., Valencia, JJ. and Szekely, J., (1992) "Fluid Flow, Heat Transfer, and Solidification of Molten Metal Droplets Impinging on Substrates: Comparison of Numerical and Experimental Results," *MetalL Trans. B.*, Vol. 23B, pp. 701-718.

Zabaras, N., Ruan, Y. and Richmond, O. (1991) "On the Calculation of Deformations and Stresses During Axially Symmetric Solidification," *Journal of Applied Mechanics,* Vol 58, pp. 865- 871.